

SLENet: A Guidance-Enhanced Network for Underwater Camouflaged Object Detection

Xinxin Huang¹, Han Sun^{1(✉)}, Ningzhong Liu¹, Huiyu Zhou², and Yinan Yao¹

¹ Nanjing University of Aeronautics and Astronautics, Nanjing, China
xxhnuaa@163.com, sunhan@nuaa.edu.cn, lnz_nuaa@163.com, yyn_nuaa@163.com

² University of Leicester, Leicester, UK
hz143@leicester.ac.uk

Abstract. Underwater Camouflaged Object Detection (UCOD) aims to identify objects that blend seamlessly into underwater environments. This task is critically important to marine ecology. However, it remains largely underexplored and accurate identification is severely hindered by optical distortions, water turbidity, and the complex traits of marine organisms. To address these challenges, we introduce the UCOD task and present DeepCamo, a benchmark dataset designed for this domain. We also propose Semantic Localization and Enhancement Network (SLENet), a novel framework for UCOD. We first benchmark state-of-the-art COD models on DeepCamo to reveal key issues, upon which SLENet is built. In particular, we incorporate Gamma-Asymmetric Enhancement (GAE) module and a Localization Guidance Branch (LGB) to enhance multi-scale feature representation while generating a location map enriched with global semantic information. This map guides the Multi-Scale Supervised Decoder (MSSD) to produce more accurate predictions. Experiments on our DeepCamo dataset and three benchmark COD datasets confirm SLENet’s superior performance over SOTA methods, and underscore its high generality for the broader COD task.

Keywords: Underwater camouflaged object detection · Multi-scale feature enhancement · Localization guidance.

1 Introduction

Detecting camouflaged objects in underwater environments presents a unique and compounded set of challenges. Beyond the inherent difficulty of identifying objects that mimic their surroundings’ color and texture, this task is further complicated by two factors: the complex characteristics of marine organisms (e.g., small size, large quantities, intricate boundaries) and severe image degradation from optical distortion and color cast. UCOD is a critical yet largely unaddressed issue for marine ecological monitoring and biodiversity conservation, with no systematic research to date in this domain. Consequently, existing general-purpose COD methods [1–8] often struggle to handle these unique underwater challenges, as shown in Fig. 1.

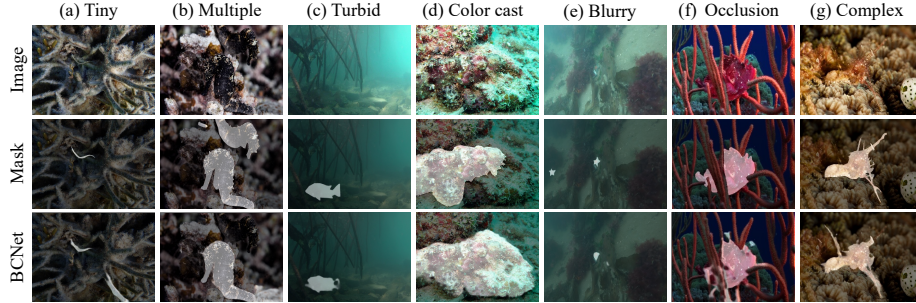


Fig. 1: Our dataset features challenging scenarios, including low-quality images (c,d,e), complex object attributes (a,b,g), and distracting backgrounds (f), where general COD methods like BCNet often suffer from missed detections or produce unclear boundaries.

Deep learning excels at COD with powerful feature extraction, surpassing traditional methods reliant on handcrafted features. Modeling complex underwater scenes requires capturing comprehensive context and long-range dependencies, yet common feature enhancement techniques often sacrifice fine details to achieve this. Models like the Segment Anything Model (SAM1) [9] and SAM2 [10] have improved segmentation performance, but their simple decoders often struggle in downstream tasks, frequently segmenting irrelevant regions. Consequently, existing COD methods often fail to precisely locate and segment small or multiple underwater objects. Furthermore, existing COD datasets [1, 11, 12] have limited diversity in underwater scenes and often overlook multi-object scenarios, which constrains model generalization and performance on UCOD tasks.

To address the above challenges, we construct DeepCamo, a dataset focused on underwater camouflaged objects in complex marine environments. Building upon the powerful encoding capability of SAM2, we propose Semantic Localization and Enhancement Network (SLENet) for the UCOD task. We use the SAM2 encoder as a backbone, freezing its pretrained weights and introducing Adapters for efficient fine-tuning. To enrich multi-scale features while preserving fine details, we introduce a cascaded Gamma-Asymmetric Enhancement (GAE) Module to enhance features at each hierarchical level. Inspired by biological hunting mechanisms, a Localization Guidance Branch (LGB) fuses multi-scale features bottom-up to generate a coarse localization map. This map then injects global localization cues into the Multi-Scale Supervised Decoder (MSSD), enabling accurate object localization. Experimental results demonstrate that SLENet significantly outperforms existing SOTA methods on the UCOD task. In summary, the main contributions of this paper are as follows:

- We conduct a systematic exploration of the UCOD task and introduce DeepCamo, a new UCOD benchmark containing 2,493 images of 16 marine species, covering diverse illumination conditions and multi-object scenarios.

- We propose the SLENet as a novel UCOD framework that effectively adapts the SAM2 encoder. It integrates the GAE to enrich features and an LGB to generate a global localization map, which in turn provides precise spatial cues to the MSSD.
- We validate each proposed module through extensive experiments, demonstrating that our SLENet consistently outperforms SOTA methods on our DeepCamo dataset and three other public COD benchmarks.

2 Related work

2.1 Camouflaged object detection

Camouflaged object detection (COD) aims to segment objects that resemble their background in color, texture, and shape. Traditional methods using hand-crafted low-level features perform adequately in simple scenes but struggle in complex environments. The availability of large-scale COD datasets [1] has enabled deep learning approaches to become mainstream. Fan et al. [1] introduced SINet, a bio-inspired CNN framework using a two-stage search-and-identify strategy. PFNet [2] employs high-level features for object localization and utilizes focus modules to reduce distractions. However, CNNs’ limited feature extraction hinders discerning subtle foreground-background differences, especially in underwater scenes with severe color bias.

Vision Transformer(ViT) [13], capable of modeling long-range dependencies and capturing global context, is a leading COD solution. FSPNet [14] employs a pyramid structure to progressively compress adjacent transformer features, accumulating informative representations. HitNet [3] introduces an iterative feedback mechanism where high-resolution features refine low-resolution representations, alleviating detail degradation. Nevertheless, Transformers require large-scale data to perform well, while underwater camouflaged images are scarce. To address this, we fine-tuning pre-trained visual foundation models to extract global features while preserving details, and incorporate localization-guided strategies to achieve accurate segmentation of underwater camouflaged objects.

2.2 Segment Anything Model for COD

Recently, SAM1 [9] demonstrated strong zero-shot image segmentation capabilities. Its successor, SAM2 [10], was trained on an expanded dataset and incorporates various enhancements. However, both models, trained on natural images, struggle with subtle foreground-background distinctions in complex underwater camouflaged scenes. To address this, many studies employ Adapters [15, 16] for parameter-efficient fine-tuning, offering domain-specific guidance. Yet, the native decoders of SAM1 and SAM2 remain too simplistic for complex tasks like COD. To improve performance, SAM2-UNet [8] integrates SAM2’s encoder into a U-Net architecture for efficient camouflage detection. Nonetheless, UCOD remains underexplored. Consequently, we propose a UCOD-oriented framework retaining SAM2’s Adapter-equipped hierarchical encoder, enabling effective capture of UCOD-specific prior knowledge.

2.3 Multi-scale Feature Enhancement

Multi-scale context is crucial in object detection, as it enhances feature representation. Hu et al. [17] thus proposed parallel pooling at various resolutions for multi-scale features. PoolNet [18] used varied downsampling rate pooling layers for multi-scale local context. While low-resolution features offer multi-scale information, they often cause detail loss. Chen et al. [19] addressed this with dilated convolutions, expanding receptive fields without extra cost or lower resolution, and developed ASPP to capture multi-scale context via varied dilation rate convolutions. Motivated by this, many COD methods adopt similar strategies. For instance, RFB [20] employed parallel dilated convolutions to expand receptive fields, mimicking human vision. However, large-dilation convolutions tend to lose fine details, challenging detection of underwater camouflaged objects with drastic scale changes. HFEM [6] captures multi-scale features via a serial multi-branch structure, avoiding large dilation rates to preserve details. However, its feature extraction and efficiency remain limited. To address this, our proposed GAE combines asymmetric and rate-2 dilated convolutions to enhance directional perception and achieve efficient multi-scale feature extraction.

3 Datasets and Benchmark Studies

3.1 Data Collection

Underwater images from common camouflage datasets often fail to capture the unique challenges of marine environments, such as color distortion, optical aberrations, and water flow effects. Moreover, these datasets lack multi-object scenarios, as the images are predominantly single-object. This data bias is a critical issue, as real marine organisms often appear in groups, which limits a model’s generalization ability to complex scenes.

To this end, we introduce DeepCamo, a UCOD dataset aptly named to reflect both the physical underwater depth and the depth of camouflage. It is curated by selecting camouflaged images from underwater datasets such as MAS3K [21], RMAS [22], and UFO120 [23], and merging them with relevant underwater scenes from the camouflage datasets CAMO [11], COD10K [1], and CHAMELEON [12].

DeepCamo’s design follows several key principles. It emphasizes seamless camouflage, making objects difficult to discern from their background, and incorporates challenging underwater environments with issues like color distortion, blur, and occlusion. Furthermore, for generalization, it ensures object diversity across species, scales, and object counts, and provides purified camouflage-only annotations by filtering ambiguous labels to focus models on true camouflage patterns.

3.2 Data Statistics

The final DeepCamo dataset contains 2,493 underwater camouflaged images covering 16 marine species. It spans diverse lighting conditions and multi-object scenarios (see Fig. 1 for examples) and is split into DeepCamo-train (1,931 images)

and DeepCamo-test (562 images) at an 8:2 ratio. Furthermore, we introduce DeepCamo-full, a benchmark subset of 1,907 images designed for fair and rigorous SOTA evaluation, which excludes all images overlapping with the COD10K training set to prevent data leakage. We hope DeepCamo will serve as a challenging and practical benchmark to advance research in UCOD.

3.3 Benchmark Study

We benchmarked 12 representative CNN-based and Transformer-based COD methods on our DeepCamo-full dataset, using their publicly available pretrained weights to ensure an objective assessment of generalization. As detailed in Table 1, all methods struggled significantly. Key localization metrics (S_α , F_β , E_ϕ) dropped by over 15%, while high MAE values indicated poor detail preservation. Even the top-performing model, SAM2-UNet, saw its MAE more than double (from 0.021 on COD10K to 0.045) and its S_α fall by 15.8%. These findings reveal the stark generalization gap of current COD methods in underwater environments, underscoring the challenge and significance of our work.

Table 1: Quantitative comparison with SOTA on DeepCamo-full (best in bold).

Category	Model	Pub./Year	$S_\alpha \uparrow$	$E_\phi \uparrow$	$F_\beta^w \uparrow$	MAE \downarrow
CNN	SINet [1]	CVPR/20	0.665	0.736	0.417	0.051
	SINet-V2 [7]	TPAMI/21	0.623	0.657	0.323	0.098
	PFNet [2]	CVPR/21	0.674	0.756	0.428	0.049
	PreyNet [24]	ACM MM/22	0.677	0.738	0.444	0.058
	BCNet [6]	Neural Comput/23	0.683	0.744	0.460	0.067
	FEDER [4]	CVPR/23	0.693	0.772	0.474	0.049
Transformer	PUENet [25]	TIP/23	0.728	0.802	0.551	0.047
	FSNet [5]	TIP/23	0.719	0.784	0.522	0.055
	HitNet [3]	AAAI/23	0.712	0.765	0.527	0.061
	Dual-SAM [26]	CVPR/24	0.692	0.732	0.484	0.058
	MAMIFNet [27]	Inf. Fusion/24	0.720	0.784	0.530	0.054
	SAM2-UNet [8]	arXiv/24	0.741	0.801	0.557	0.045

4 Method

UCOD is hindered by the loss of fine-grained details during multi-scale feature extraction and by inaccurate localization, which impairs the detection of small or multiple objects. To address these challenges, we propose SLENet (Fig. 2), consisting of four key modules namely the SAM2 encoder with Adapters, the Gamma-Asymmetric Enhancement (GAE) module, the Localization Guidance Branch (LGB), and the Multi-Scale Supervised Decoder (MSSD). The following sections describe the design of each module and the overall loss function.

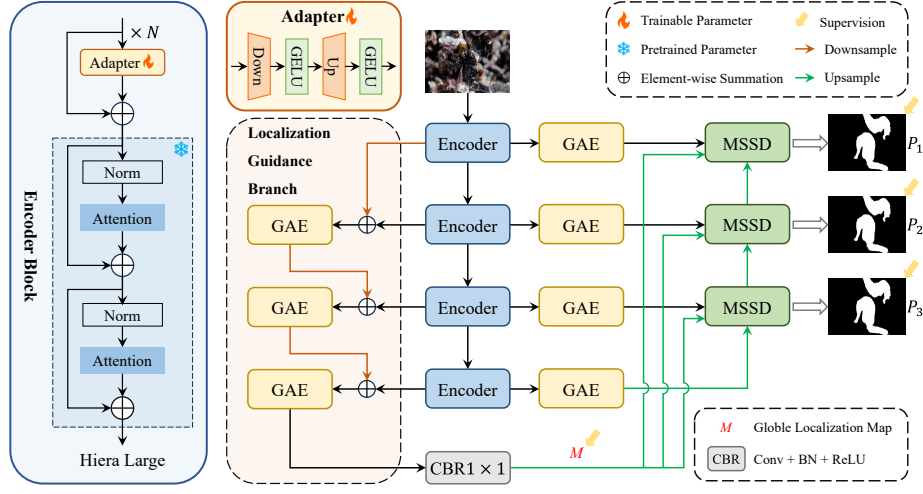


Fig. 2: The overall architecture of SLENet is composed of four key components: a SAM encoder with an Adapter, a Gamma-Asymmetric Enhancement (GAE) module, a Localization Guidance Branch (LGB), and a Multi-Scale Supervised Decoder (MSSD).

4.1 SAM2 Encoder with Adapter

To mitigate SAM2’s tendency to produce category-irrelevant segmentations without manual prompts, we employ lightweight Adapters for parameter-efficient fine-tuning, injecting domain-specific knowledge for underwater camouflage. The backbone of SLENet adopts SAM2’s Hiera-L encoder. While Hiera-L’s parameters are frozen, we insert a trainable Adapter before each block to enable domain-specific tuning while capturing long-range context. Following established practices [15, 16], each Adapter consists of a linear layer for downsampling, a GeLU activation, another linear layer for upsampling, and another GeLU activation. This Adapter-equipped encoder then extracts four levels of multi-scale features from an input image.

4.2 Gamma-Asymmetric Enhancement Module

To enhance multi-scale feature perception while preserving critical details, we propose the GAE Module. For each input feature $X_i, i \in \{1, 2, 3, 4\}$, GAE employs four sequential branches. Each branch contains a 1×1 channel-reduction convolution, asymmetric convolutions to reduce parameter redundancy and enhance directional sensitivity, max-pooling layers, and a dilated convolution with a dilation rate of 2 to capture long-range dependencies. The output of each branch after channel compression is denoted as $X_i^r, r \in \{1, 2, 3, 4\}$, where r is the branch index. For progressive enhancement, each subsequent branch contains fewer subsampling layers and receives the concatenated output of the previous

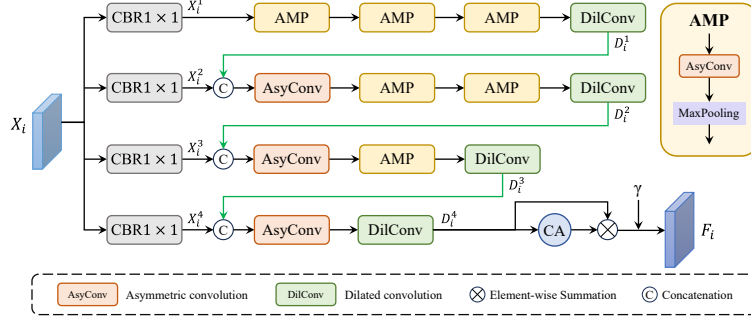


Fig. 3: The architecture of Gamma-Asymmetric Enhancement (GAE) module.

branch as part of its input. This design expands the receptive field while integrating high-resolution features from earlier stages, thus enriching context and recovering fine details. The complete formulation for each branch is as follows:

$$D_i^1 = C_{dil}(AMP_{\times 3}(X_i^1)), \quad (1)$$

$$C_i^r = C_{asy}(Cat(X_i^r, Up(D_i^{r-1}, X_i^r))), \quad r = 2, 3, 4, \quad (2)$$

$$D_i^r = C_{dil}(AMP_{\times (4-r)}(C_i^r)), \quad r = 2, 3, 4, \quad (3)$$

where C_{dil} and C_{asy} denote dilated convolution and asymmetric convolution, respectively. $AMP_{\times N}$ denotes N pairs of asymmetric convolution and max-pooling layers. $Up(D_i^{r-1}, X_i^r)$ refers to upsampling D_i^{r-1} to the spatial size of X_i^r , and Cat denotes concatenation. The feature D_i^4 is processed by a channel attention mechanism to enhance discriminative semantic channels. Then, a learnable scaling factor γ is introduced to adaptively adjust weights based on contextual information, enhancing both performance and stability. The final enhanced feature is thus obtained as:

$$F_i = \gamma(D_i^4 \otimes CA(D_i^4)), \quad (4)$$

where CA is channel attention and \otimes denotes element-wise multiplication.

4.3 Localization Guidance Branch

The Localization Guidance Branch (LGB) fuses cross-scale features in a bottom-up manner to refine the model's localization capabilities. Initially, the multi-scale features extracted from the backbone are compressed to a unified channel dimension via 1×1 convolutions and are denoted as X_i^l . Starting from the shallowest feature, each is fused with the adjacent deeper feature, then enhanced by the GAE module for improved contextual awareness. This enhanced output then serves as the input for the next fusion, as described by:

$$F_2^l = GAE(Down(X_1^l) \oplus X_2^l), \quad (5)$$

$$F_i^l = GAE(Down(F_{i-1}^l) \oplus X_i^l), \quad i = 3, 4, \quad (6)$$

where *Down* is downsampling, and \oplus denotes element-wise summation. This iterative fusion process enables the LGB to effectively aggregate rich multi-scale semantic representations. The final feature F_4^l is then processed by a 1×1 convolution to produce a coarse localization map M with lower spatial resolution but stronger semantic representation:

$$M = CBR_{1 \times 1}(F_4^l), \quad (7)$$

where $CBR_{N \times N}$ signifies a sequence of $N \times N$ convolution, batch normalization and ReLU.

4.4 Multi-Scale Supervised Decoder

To enhance spatial awareness and focusing capabilities, the MSSD (Fig. 4) performs a top-down, iterative cross-scale fusion. It takes the GAE-enhanced features F_i and the previous stage's output R_{i+1} as input, and leverages the global localization map M to achieve focus. Specifically, higher-level features are up-sampled and concatenated with the current layer features F_i along the channel dimension, then further fused through two consecutive 3×3 convolutional blocks to produce S'_i . This process is described as:

$$S_i = \text{Cat}(F_i, \text{Up}(R_{i+1}, F_i)), \quad i = 1, 2, \quad (8)$$

$$S_3 = \text{Cat}(F_3, \text{Up}(F_4, F_3)), \quad (9)$$

$$S'_i = CBR_{3 \times 3}(CBR_{3 \times 3}(S_i)), \quad i = 1, 2, 3. \quad (10)$$

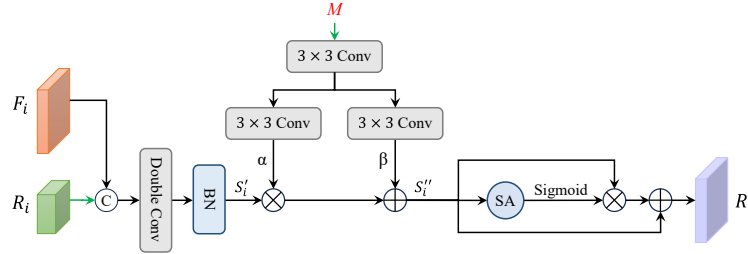


Fig. 4: The architecture of Multi-Scale Supervised Decoder (MSSD).

The localization map M serves as guidance for the feature modulation. It is first upsampled to match the feature resolution of S'_i and then processed through two parallel 3×3 convolutional blocks to generate a scale factor α and shift factor β . These affine parameters are integrated into the normalization of the fused feature S'_i [28], enabling the following modulation:

$$S''_i = BN(S'_i) \otimes \alpha(M) \oplus \beta(M), \quad (11)$$

where BN denotes batch normalization. A spatial attention block is then introduced to further enhance salient regions. The modulated features are combined

with the weighted features via residual connection to produce the output R_i . The final segmentation result P_i is obtained by applying a 1×1 convolution to R_i . This process is formulated as:

$$R_i = (\text{Sigmoid}(SA(S_i'')) \otimes S_i'') \oplus S_i'', \quad P_i = \text{Conv}_{1 \times 1}(R_i), \quad (12)$$

where SA denotes spatial attention, and $\text{Conv}_{1 \times 1}$ represents a 1×1 convolutional layer.

4.5 Loss Function

To mitigate the model’s bias towards the background in class-imbalanced segmentation, we employ a weighted binary cross-entropy (wBCE) loss, with weights adaptively assigned based on pixel contrast. To further enhance global structure modeling, we incorporate a similarly weighted IoU loss, yielding the combined loss function $\mathcal{L} = \mathcal{L}_{BCE}^w + \mathcal{L}_{IOU}^w$.

The map M is also supervised by an independent binary cross-entropy (BCE) loss. While this map provides crucial global guidance early in training, a persistently high loss weight can cause an over-reliance on its coarse representation, impeding the learning of fine-grained details. To mitigate this, we employ a linear decay strategy to dynamically adjust the weight of the M branch. The specific weight and the final combined loss are defined as follows:

$$\omega_m = \max(\mu(1 - \frac{epoch}{epochs}), 0.1), \quad (13)$$

$$\mathcal{L}_{total} = \omega_m \mathcal{L}_{BCE}(G, M) + \frac{1 - \omega_m}{3} \sum_{i=1}^3 \mathcal{L}(G, P_i), \quad (14)$$

the weight ω_m decays linearly from an initial value μ to 0.1 as the current epoch ($epoch$) progresses towards the total epochs ($epochs$). G denotes ground truth.

5 Experiments

5.1 Experimental Setup

Our model is implemented in PyTorch and trained on a single RTX 4090 GPU. We employ the AdamW optimizer with an initial learning rate of $5e-4$, which decays following a cosine schedule. The backbone is the Hiera-L encoder from SAM2. All images are resized to 352×352 and processed with a batch size of 16 for 100 epochs. The weight parameter μ is set to 0.6. To evaluate our method, we conduct experiments on our proposed DeepCamo dataset and three public benchmarks, including CAMO [11], CHAMELEON [12], and COD10K [1]. Performance is assessed using five metrics: S-measure (S_α), weighted F-measure (F_β^w), mean E-measure (E_ϕ), and mean absolute error (MAE).

Table 2: Quantitative results on four benchmark datasets. “ \uparrow / \downarrow ” indicates that larger or smaller is better. The best and second-best results are represented in bold and with an underline, respectively.

Models	DeepCamo-Test				COD10K-Test			
	$S_\alpha \uparrow$	$E_\phi \uparrow$	$F_\beta^w \uparrow$	MAE \downarrow	$S_\alpha \uparrow$	$E_\phi \uparrow$	$F_\beta^w \uparrow$	MAE \downarrow
SINet [1]	0.745	0.803	0.501	0.057	0.771	0.806	0.551	0.051
SINet-V2 [7]	0.806	0.886	0.694	0.039	0.815	0.887	0.680	0.037
PFNet [2]	0.805	0.880	0.690	0.041	0.800	0.868	0.660	0.040
BCNet [6]	0.815	0.897	0.716	0.035	0.837	0.894	0.704	0.033
FSNet [5]	0.847	0.920	0.765	0.027	0.870	<u>0.938</u>	0.810	0.023
HitNet [3]	0.852	0.922	<u>0.778</u>	0.030	0.868	0.932	0.798	0.024
PUNet [25]	0.840	0.913	0.770	0.032	0.873	<u>0.938</u>	<u>0.812</u>	0.022
Dual-SAM [26]	0.819	0.873	0.733	0.034	0.832	0.893	0.754	0.027
MAMIFNet [27]	0.855	<u>0.925</u>	0.774	0.028	0.869	0.933	0.785	0.023
SAM2-UNet [8]	<u>0.859</u>	0.919	0.767	<u>0.025</u>	<u>0.880</u>	0.936	0.789	<u>0.021</u>
SLENet(Ours)	0.869	0.930	0.800	0.022	0.883	0.945	0.820	0.019

Models	CAMO-Test				CHAMELEON			
	$S_\alpha \uparrow$	$E_\phi \uparrow$	$F_\beta^w \uparrow$	MAE \downarrow	$S_\alpha \uparrow$	$E_\phi \uparrow$	$F_\beta^w \uparrow$	MAE \downarrow
SINet [1]	0.751	0.771	0.606	0.100	0.869	0.891	0.740	0.044
SINet-V2 [7]	0.820	0.882	0.743	0.070	0.888	0.942	0.816	0.030
PFNet [2]	0.782	0.852	0.695	0.085	0.882	0.942	0.810	0.033
BCNet [6]	0.830	0.886	0.761	0.068	0.901	0.944	0.839	0.029
FSNet [5]	0.880	<u>0.933</u>	0.861	<u>0.041</u>	0.905	0.963	0.868	0.022
HitNet [3]	0.844	0.903	0.801	0.057	<u>0.922</u>	<u>0.970</u>	0.903	<u>0.018</u>
PUNet [25]	0.877	0.930	<u>0.860</u>	0.045	0.910	0.957	0.869	0.022
Dual-SAM [26]	0.825	0.885	0.787	0.058	0.807	0.877	0.731	0.048
MAMIFNet [27]	0.872	0.929	0.834	0.045	0.914	0.960	0.875	0.021
SAM2-UNet [8]	<u>0.884</u>	0.932	0.861	0.042	0.914	0.961	0.863	0.022
SLENet(Ours)	0.887	0.937	<u>0.860</u>	0.039	0.923	0.973	<u>0.896</u>	0.017

5.2 Comparison with SOTA Methods

Our method is compared with 10 state-of-the-art COD approaches, including SINet [1], SINet-V2 [7], PFNet [2], BCNet [6], FSNet [5], HitNet [3], PUNet [25], Dual-SAM [26], MAMIFNet [27], and SAM2-UNet [8], on both the DeepCamo dataset and COD benchmark datasets.

Quantitative comparison. Table 2 summarizes the quantitative comparison of SLENet against SOTA methods on our DeepCamo dataset and three public benchmarks. SLENet consistently outperforms all competing CNN-based and Transformer-based methods across all evaluation metrics. This superiority is particularly evident on our challenging DeepCamo dataset, which features highly camouflaged objects and strong background interference. Here, SLENet surpasses the runner-up, SAM2-UNet, improving S_α and F_β^w by 1.2% and 4.3%

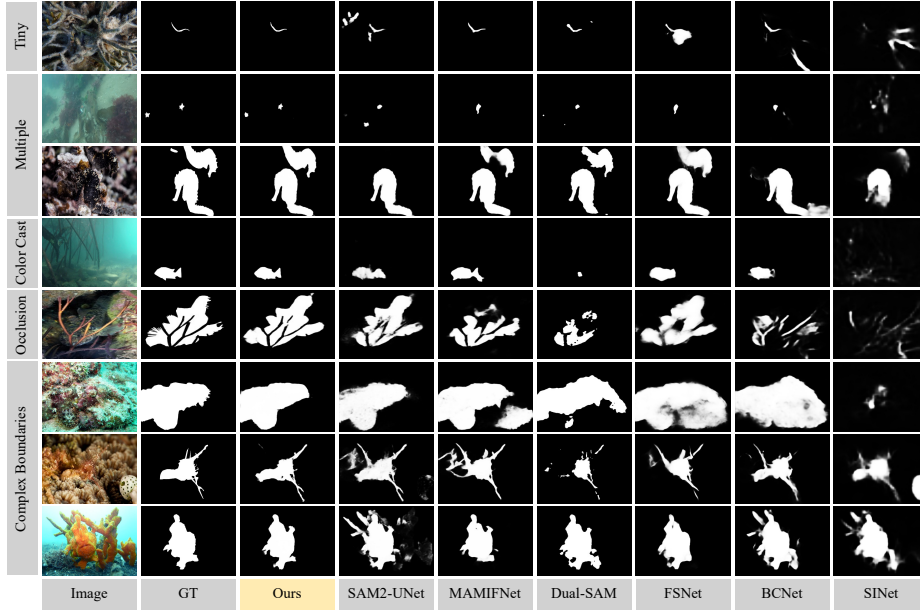


Fig. 5: Qualitative comparisons of the SLENet with several SOTA methods.

Table 3: Ablation studies on the DeepCamo dataset. “G” , “L” , and “M” denote GAE, LGB, and MSSD, respectively.

(a) Ablation results of each module.							(b) Results with different μ .				
G	L	M	$S_\alpha \uparrow$	$E_\phi \uparrow$	$F_\beta^w \uparrow$	MAE \downarrow	μ	$S_\alpha \uparrow$	$E_\phi \uparrow$	$F_\beta^w \uparrow$	MAE \downarrow
✓	✓	✓	0.858	0.918	0.764	0.026	0.2	0.868	0.929	0.796	0.023
			0.864	0.928	0.784	0.023	0.4	0.866	0.928	0.795	0.023
			0.864	0.920	0.791	0.024	0.6	0.869	0.930	0.800	0.022
✓	✓	✓	0.869	0.930	0.800	0.022	0.8	0.865	0.924	0.791	0.022

respectively, while decreasing the MAE by 12%. Notably, achieving stable performance gains on a highly challenging dataset demonstrates the robustness of our model. Moreover, this strong performance extends to established benchmarks like COD10K, where SLENet achieves a 9.5% reduction in MAE compared to SAM2-UNet. These consistent gains across diverse datasets underscore the effectiveness and strong generalization capabilities of SLENet.

Qualitative comparison. Fig. 5 showcases the qualitative performance of SLENet on representative samples from various test sets. These samples cover challenging scenarios, including small or multiple objects, occlusion, and poor visibility due to distortion or turbidity. Across these complex scenes, SLENet

accurately identifies object regions and delineates their boundaries with high precision. In contrast, many SOTA methods struggle with such cases, often yielding missed detections or blurred edges. By incorporating the GAE and LGB modules, our model effectively reconstructs fine-grained details and improves localization accuracy, yielding predictions that closely match the ground truth. This visual evidence clearly demonstrates the superiority of SLENet over existing approaches.

5.3 Ablation Study

Impact of key components. Ablation studies on DeepCamo (Table 3a) assess the impact of key components (GAE, LGB, and MSSD) by removing them from the full model.

- **Effectiveness of GAE.** A baseline model using only plain convolutions performs the worst. Adding GAE significantly enhances context extraction and detail modeling, improving F_β^w by 2.6% and reducing MAE by 11.5%. This demonstrates its ability to capture fine boundary and texture details.
- **Effectiveness of LGB & MSSD.** LGB offers global localization guidance. Combined with MSSD for multi-scale fusion, it improves localization and structural consistency, yielding a 3.5% F_β^w gain over the baseline.
- **Effectiveness of full model.** The full model achieves top performance across all metrics, confirming their synergistic contributions to precise localization and context-aware representation in complex environments.

Impact of μ . We analyze the impact of μ , the initial loss weight for the LGB’s global localization map M (Table 3b). When $\mu = 0$, the M branch weight is fixed at a low 0.1, providing minimal guidance and leading to a significant performance drop. This result is omitted from the table to better illustrate the key trend. As μ increases, enhanced global guidance improves object localization, with optimal performance achieved at $\mu = 0.6$. However, excessively high μ values cause over-reliance on global supervision, thereby hindering fine-grained feature learning and degrading performance.

6 Conclusion

In this work, we present a comprehensive study of the challenging task of underwater camouflaged object detection. To facilitate research in this underexplored domain, we introduce DeepCamo, a benchmark dataset tailored for UCOD, which establishes a foundational benchmark. We also propose SLENet, a novel framework tailored to the unique challenges of underwater camouflage. SLENet introduces the GAE module to enhance features across all scales, significantly improving detail and texture modeling. Building on this, the LGB and MSSD modules work in concert to provide global localization modulation and cross-scale feature fusion. Extensive experiments on DeepCamo and three general

COD datasets validate that SLENet achieves SOTA performance, demonstrating excellent robustness and generalization. We believe this work provides a solid foundation for future UCOD research, with promising directions including underwater image enhancement and cross-domain adaptation.

References

1. Fan, D.P., Ji, G.P., Sun, G., Cheng, M.M., Shen, J., Shao, L.: Camouflaged object detection. In: Proceedings of the IEEE/CVF conference on computer vision and pattern recognition. pp. 2777–2787 (2020)
2. Mei, H., Ji, G.P., Wei, Z., Yang, X., Wei, X., Fan, D.P.: Camouflaged object segmentation with distraction mining. In: Proceedings of the IEEE/CVF conference on computer vision and pattern recognition. pp. 8772–8781 (2021)
3. Hu, X., Wang, S., Qin, X., Dai, H., Ren, W., Luo, D., Tai, Y., Shao, L.: High-resolution iterative feedback network for camouflaged object detection. In: Proceedings of the AAAI Conference on Artificial Intelligence. vol. 37, pp. 881–889 (2023)
4. He, C., Li, K., Zhang, Y., Tang, L., Zhang, Y., Guo, Z., Li, X.: Camouflaged object detection with feature decomposition and edge reconstruction. In: Proceedings of the IEEE/CVF conference on computer vision and pattern recognition. pp. 22046–22055 (2023)
5. Song, Z., Kang, X., Wei, X., Liu, H., Dian, R., Li, S.: Fsnet: Focus scanning network for camouflaged object detection. *IEEE Transactions on Image Processing* **32**, 2267–2278 (2023)
6. Xiao, J., Chen, T., Hu, X., Zhang, G., Wang, S.: Boundary-guided context-aware network for camouflaged object detection. *Neural Computing and Applications* **35**(20), 15075–15093 (2023)
7. Fan, D.P., Ji, G.P., Cheng, M.M., Shao, L.: Concealed object detection. *IEEE transactions on pattern analysis and machine intelligence* **44**(10), 6024–6042 (2021)
8. Xiong, X., Wu, Z., Tan, S., Li, W., Tang, F., Chen, Y., Li, S., Ma, J., Li, G.: Sam2-unet: Segment anything 2 makes strong encoder for natural and medical image segmentation. *arXiv preprint arXiv:2408.08870* (2024)
9. Kirillov, A., Mintun, E., Ravi, N., Mao, H., Rolland, C., Gustafson, L., Xiao, T., Whitehead, S., Berg, A.C., Lo, W.Y., et al.: Segment anything. In: Proceedings of the IEEE/CVF international conference on computer vision. pp. 4015–4026 (2023)
10. Ravi, N., Gabeur, V., Hu, Y.T., Hu, R., Ryali, C., Ma, T., Khedr, H., Rädle, R., Rolland, C., Gustafson, L., et al.: Sam 2: Segment anything in images and videos. *arXiv preprint arXiv:2408.00714* (2024)
11. Le, T.N., Nguyen, T.V., Nie, Z., Tran, M.T., Sugimoto, A.: Anabran network for camouflaged object segmentation. *Computer vision and image understanding* **184**, 45–56 (2019)
12. Skurowski, P., Abdulameer, H., Błaszczyk, J., Depta, T., Kornacki, A., Koziel, P.: Animal camouflage analysis: Chameleon database. Unpublished manuscript **2**(6), 7 (2018)
13. Dosovitskiy, A., Beyer, L., Kolesnikov, A., Weissenborn, D., Zhai, X., Unterthiner, T., Dehghani, M., Minderer, M., Heigold, G., Gelly, S., et al.: An image is worth 16x16 words: Transformers for image recognition at scale. *arXiv preprint arXiv:2010.11929* (2020)

14. Huang, Z., Dai, H., Xiang, T.Z., Wang, S., Chen, H.X., Qin, J., Xiong, H.: Feature shrinkage pyramid for camouflaged object detection with transformers. In: Proceedings of the IEEE/CVF conference on computer vision and pattern recognition. pp. 5557–5566 (2023)
15. Hounsby, N., Giurigu, A., Jastrzebski, S., Morrone, B., De Laroussilhe, Q., Gesmundo, A., Attariyan, M., Gelly, S.: Parameter-efficient transfer learning for nlp. In: International conference on machine learning. pp. 2790–2799. PMLR (2019)
16. Qiu, Z., Hu, Y., Li, H., Liu, J.: Learnable ophthalmology sam. arXiv preprint arXiv:2304.13425 (2023)
17. Hu, H., Bai, S., Li, A., Cui, J., Wang, L.: Dense relation distillation with context-aware aggregation for few-shot object detection. In: Proceedings of the IEEE/CVF conference on computer vision and pattern recognition. pp. 10185–10194 (2021)
18. Liu, J.J., Hou, Q., Cheng, M.M., Feng, J., Jiang, J.: A simple pooling-based design for real-time salient object detection. In: Proceedings of the IEEE/CVF conference on computer vision and pattern recognition. pp. 3917–3926 (2019)
19. Chen, L.C., Papandreou, G., Kokkinos, I., Murphy, K., Yuille, A.L.: Deeplab: Semantic image segmentation with deep convolutional nets, atrous convolution, and fully connected crfs. *IEEE transactions on pattern analysis and machine intelligence* **40**(4), 834–848 (2017)
20. Wu, Z., Su, L., Huang, Q.: Cascaded partial decoder for fast and accurate salient object detection. In: Proceedings of the IEEE/CVF conference on computer vision and pattern recognition. pp. 3907–3916 (2019)
21. Li, L., Rigall, E., Dong, J., Chen, G.: Mas3k: An open dataset for marine animal segmentation. In: International Symposium on Benchmarking, Measuring and Optimization. pp. 194–212. Springer (2020)
22. Fu, Z., Chen, R., Huang, Y., Cheng, E., Ding, X., Ma, K.K.: Masnet: A robust deep marine animal segmentation network. *IEEE Journal of Oceanic Engineering* (2023)
23. Islam, M.J., Luo, P., Sattar, J.: Simultaneous enhancement and super-resolution of underwater imagery for improved visual perception. arXiv preprint arXiv:2002.01155 (2020)
24. Zhang, M., Xu, S., Piao, Y., Shi, D., Lin, S., Lu, H.: Preynet: Preying on camouflaged objects. In: Proceedings of the 30th ACM international conference on multimedia. pp. 5323–5332 (2022)
25. Zhang, Y., Zhang, J., Hamidouche, W., Deforges, O.: Predictive uncertainty estimation for camouflaged object detection. *IEEE Transactions on Image Processing* **32**, 3580–3591 (2023)
26. Zhang, P., Yan, T., Liu, Y., Lu, H.: Fantastic animals and where to find them: Segment any marine animal with dual sam. In: Proceedings of the IEEE/CVF Conference on Computer Vision and Pattern Recognition. pp. 2578–2587 (2024)
27. Wang, T., Yu, Z., Fang, J., Xie, J., Yang, F., Zhang, H., Zhang, L., Du, M., Li, L., Ning, X.: Multidimensional fusion of frequency and spatial domain information for enhanced camouflaged object detection. *Information Fusion* **117**, 102871 (2025)
28. Park, T., Liu, M.Y., Wang, T.C., Zhu, J.Y.: Semantic image synthesis with spatially-adaptive normalization. In: Proceedings of the IEEE/CVF conference on computer vision and pattern recognition. pp. 2337–2346 (2019)